Towards Attosecond X-Ray Pulses from the FEL

Alexander A. Zholents, William M. Fawley, LBNL, Berkeley, CA 94720-8211, USA

INTRODUCTION

The ability to study ultrafast phenomena has been recently advanced by the demonstrated production and measurement of a single, 650-attosecond (10^{-18} sec), VUV x-ray pulse[1] and, latter, a 250-attosecond pulse[2]. The next frontier is a production of the x-ray pulses with a shorter wavelengths and in a broader spectral range. Several techniques for a generation of an isolated, attosecond duration, short-wavelength x-ray pulse based upon the ponderomotive laser acceleration [3], SASE and harmonic cascade FELs ([4] - [6]) had been already proposed. In this paper we briefly review a technique proposed in [5] and present some new results.

METHOD AND ILLUSTRATIONS

Generation of attoseond x-ray pulses in [5] requires an ultra-relativistic electron beam, a few-cycle, intense optical laser pulse and an intense pulse of the coherent x-ray radiation, together with a number of magnetic undulators and transport elements. Fig.1 schematically shows how all these components are used. On the left is a source producing a coherent 2-nm wavelength, $\sim 100-$fs, $\sim 100-$MW peak power x-ray pulses. While such sources do not exist today, studies of harmonic cascade FEL's (HC FEL) ([7] -[9]) have suggested approaches which are feasible in principle. HC FEL can be configured such that only part of the electron bunch is used for the x-ray generation, thus leaving another part near the bunch head whose instantaneous energy spread σ_E has not been degraded by previous FEL interaction in the upstream cascade or even by SASE gain.

After exiting the HC FEL, an achromatic bend inserts the electrons into a two-period wiggler magnet "800-nm modulator". Simultaneously, a 800-nm wavelength, ~ 1 mJ, 5-fs laser pulse enters this wiggler and co-propagates with the electrons. The technical feasibility of such optical pulses has already been proven[10]. The relative timing between the arrival of the electron beam and the optical pulse is set such that the latter temporally overlaps "virgin" electrons. We presume that the x-ray HC FEL pulse will be seeded with a laser pulse which originates from the same laser source as the few-cycle laser pulse which consequently permits tight synchronization between the two. Since the "virgin" ultra-relativistic electrons and the HC FEL x-ray pulse come from the same electron bunch, one can thus ensure temporal synchronization between each of these three beams.

The carrier-envelope phase of the few-cycle laser pulse is adjusted so that the peak electric field appears at the peak of the envelope when the laser pulse passes the wiggler center. The wiggler's magnetic period and undulator parameter K are adjusted such that fundamental FEL resonance occurs at the laser wavelength $\lambda_L = 800$ nm. The interaction with the laser light in the wiggler then produces a time-dependent electron energy modulation extended over few optical cycles. For the laser pulse parameters mentioned above, we expect a central peak energy offset $\Delta \mathcal{E}_o \approx 15$ MeV which is a factor of 1.35 times larger than those of its two nearest neighbors. This relative difference is important when considering the 2-nm energy modulation to be induced in a following undulator.

A second isochronous bend after the wiggler magnet returns the electrons back to the original axis. The electrons now enter a long undulator-modulator (UM) (not shown to scale in Fig. 1), which serves as an energy modulator at 2-nm wavelength. The coherent, $\geq 100-$fs long, 2-nm output pulse from the HC FEL co-propagates in the UM with electrons and arrives simultaneously with those electrons that experienced the strong energy modulation at 800 nm. The undulator parameter K of the UM is tuned such that only those electrons very near the peak of the 800-nm energy modulation have the correct energy for resonant FEL interaction with the 2-nm light. The other electrons fall outside the energy bandwidth of the UM and are not significantly modulated. The UM is shorter than one full FEL gain length so there is little SASE action leading to unwanted microbunching at 2-nm wavelength throughout the 2-ps long electron bunch.

Downstream of the UM the electrons enter a chicane which induces strong microbunching at $\lambda_x = 2$-nm wavelength and at higher harmonics λ_x/n. In Fig. 2 we plot the bunching amplitude for $n = 2$ (*i.e.* 1-nm wavelength) as predicted using Eq.5 of Ref.[5] and as calculated by the GINGER simulation code [11].

After the chicane, the electrons proceed to an undulator-radiator (UR) in micro-bunches and produce coherent emission at wavelength $\lambda_x/n = 1$ nm. The interference of the waves emitted by all macroparticles defines the output envelope of the radiation field. The predicted radiation field intensity is shown in Fig. 3. The rms width σ_t of the peak is 48 attoseconds for the radiator with a number of periods $N_R = 80$ and 75 attoseconds for the radiator with $N_R = 45$. This is several times shorter than the bunching width structure shown in Fig. 2. We attribute this reduction to a destructive interference (due to temporal variation of bunching phase) occurring between waves emitted by microbunches on opposite sides of the bunching peak.
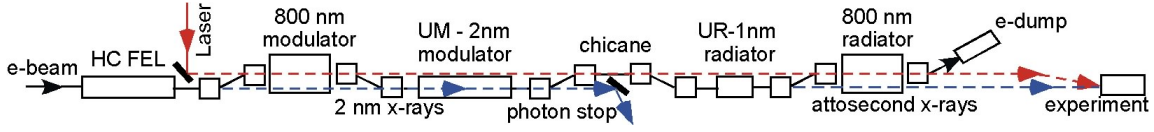
Figure 1: A schematic of the components involved in attosecond x-ray pulse production.
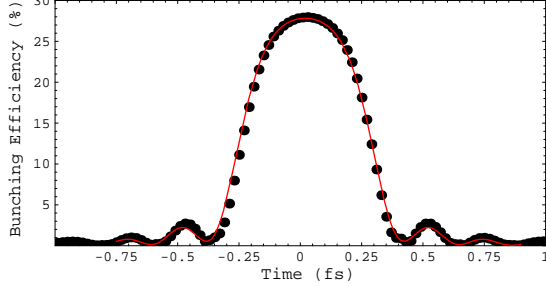

Figure 2: Bunching efficiency at 1-nm wavelength versus time along the electron bunch. The solid line shows analytical prediction and the dots simulation results from GINGER. The FWHM of the peak is 530 attoseconds.
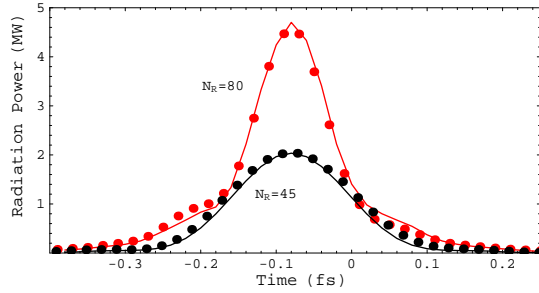

Figure 3: Predicted attosecond pulse power at 1-nm wavelength from a radiator with $N_R = 80$ (top line) and $N_R = 45$ (bottom line). Both curves were normalized to the peak intensity of the $N_R = 80$ simulation results (dots).
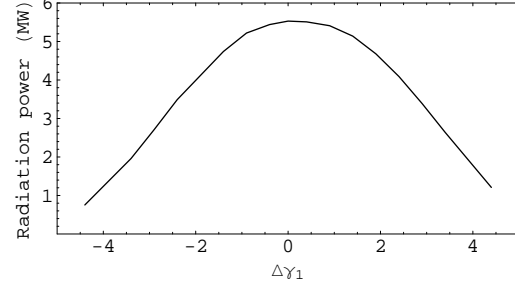

Figure 4: Predicted peak radiated power versus detuning from the FEL resonance energy in the UM.
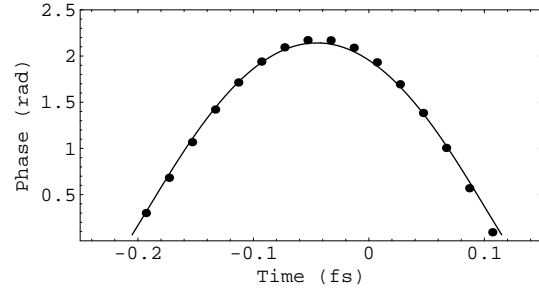

Figure 5: Predicted attosecond pulse phase at 1-nm wavelength from a radiator with 45 periods. The line shows analytical calculation while the dots show GINGER simulation results.

We also plot in Fig. 4 the dependence of the peak radiation power as the function of the detuning $\Delta\gamma_1$ of the electron beam energy from the FEL resonance energy in the UM.

There is another interesting phenomenon related to interference effects, namely the variation of the output electric field phase Ψ with time. Fig. 5 shows this variation for $N_R = 45$ fitted by a parabola $\Psi(t) = a(t/\sigma_t)^2$ with $a = 1.92$. The quadratic component indicates a frequency chirp and, thus, a time-bandwidth product exceeding the ultimate Fourier transform limit by a factor $\sqrt{1 + a^2}$ [12]. Consequently, the output pulse for the bottom curve in Fig. 3 could potentially be compressed down to $\tilde{\sigma}_t = \sigma_t/\sqrt{1 + a^2} = 35$ attoseconds. We found, that the variation of $\Delta\gamma_1$ from -3 to 3 causes only $\sim 20\%$ variation in a. For a longer radiator, the frequency chirp lessens and effectively disappears by $N_R = 80$.

Fig. 6 shows the output spectra corresponding to both the coherent attosecond radiation and incoherent spontaneous emission. In this example the coherent radiation is constrained within a rms solid angle of $\sim 3 \times 10^{-11}$ sr. Spontaneous radiation is emitted into a solid angle approximately two orders of magnitude larger. The two spectra are also shifted in wavelength with respect to each other by about 1%. The shift is due to the different energy of microbunched electrons. and can be increased by the use of a more intense laser. One may also consider to modify the temporal dependence of the primary energy modulation in the wiggler magnet and obtain more than a single attosecond pulse separated by a short (few femtosecond) time intervals. For example one could shift the phase of the laser pulse entering the wiggler magnet by 180 degrees and obtain *two* attosecond output x-ray pulses separated exactly by one period of the optical cycle as shown in Fig. 7.

Presently there exist several design studies for x-ray facilities based upon harmonic cascade FELs: LBNL LUX[13], BESSY FEL[14], MIT-BATES FEL[15]. The scheme described above can be added to any of them with a relatively modest effort as compared to what would be required to build a primary facility. The physical addition of this scheme would not require any other significant change
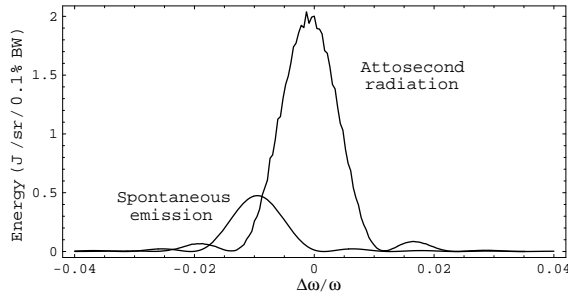
Figure 6: The predicted on-axis, far-field radiation spectrum $d^2P/d\Omega\,d\omega$ at 1-nm wavelength from a radiator with 80 periods. The attosecond output was calculated by the GINGER code whereas the spontaneous emission curve is an analytic result for a presumed e-beam pulse duration of 2 ps.
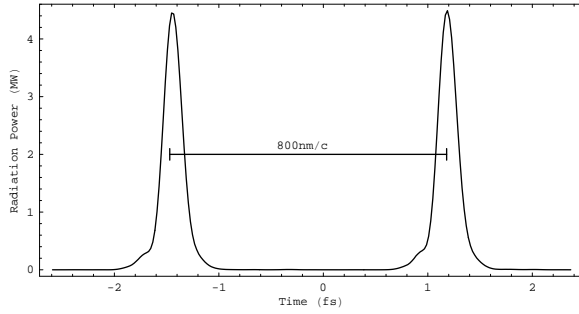

Figure 7: Predicted instantaneous output power by the GINGER code for the case in which the phase of the intense optical pulse has been shifted 180 degrees (effectively reversing the sign of the energy modulation used previously).

or improvement in the ways these facility will operate. We demonstrated this by purposely choosing for our illustrative example exactly the same electron beam and x-ray light parameters as are currently considered in the LUX's studies.

In the above example we choose 2 nm as the x-ray source wavelength to eventually produce 1-nm wavelength attosecond radiation. However, as long as an intense, coherent source is available, attosecond pulse generation at both longer and shorter wavelengths is also possible with the same scheme. For example, the interaction of intense laser pulse with noble gases produces a highly coherent light at high-order harmonics of the laser frequency. A submicrojoule pulse at the wavelength around 30 nm had been already demonstrated[16]. Naturally, such a source can be used instead of HC FEL. In the following illustrative example we assume that 200 nJ, 10 fs pulse at 32 nm wavelength co-propagates the UM with a 1.5 GeV electron beam that already passed the wiggler and experienced an energy modulation by a 2 μm few-cycle laser pulse[17] with a peak amplitude achieving 7.5 MeV. The UM has 50 periods and the period of 4 cm. The undulator parameter K of the UM is now tuned for resonant FEL interaction with the 32-nm light for electrons at the peak of the 2 μm
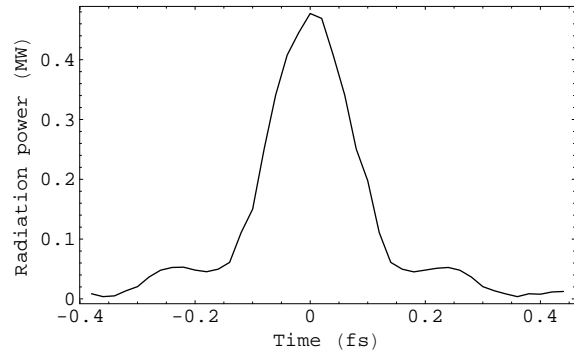

Figure 8: Estimated attosecond pulse power at 4-nm wavelength from a radiator with $N_R = 25$.

energy modulation. This interaction produces energy modulation with $\sim$0.5 MeV amplitude, which is much larger than 20 keV rms beam energy spread assumed in this example. This allows to obtain a significant bunching at 4 nm wavelength considered here and even shorter wavelengths. The estimated attosecond pulse produced by the bunched electrons in the UR consisting of 25 period with period length of 2 cm is shown in Fig. 8. In all these calculations we assumed the electron peak current of 100 A and the normalized electron beam emittance of 1 mm-mrad.

REFERENCES

[1] M. Hentchel et al. , Nature, **416**, 509 (2001).

[2] R. Kienberger et al. , Nature, **427**, 817 (2004).

[3] M. Zolotorev, NIM A, , **483**, 445 (2002).

[4] E.L. Saldin et al. , Opt. Comm., **212**, 377 (2002).

[5] A.A. Zholents, W.M. Fawley, Phys. Rev. Lett., **92**, 224801 (2004); LBNL-54084Ext, (2003).

[6] E.L. Saldin et al. , DESY 04-013, (2004), submitted to Opt. Comm.

[7] L.-H. Yu et al. , Science, **289**, 932 (2000).

[8] G. Penn et al. , this conf., MOPKF074.

[9] W. Fawley et al. , Proc. 2003 Part. Acc. Conf., 923 (2003).

[10] S. Sartania et al. , Opt. Lett., **22**, 1562 (1997).

[11] W.M. Fawley, LBNL Tech. Rpt. 49625, (2001).

[12] J.-C. Diels and W. Rudolph, Ultrashort Laser Phenomena, Academic Press, (1996).

[13] J.N. Corlett et al. , this conf., THPKF075.

[14] M. Abo-Bakr et al. , NIM A, **483**, 470 (2002).

[15] D.E. Moncton and W.S. Graves, Proc. 2003 Synchr. Rad. Instr. Conf., San Francisco (2003).

[16] E. Takahashi et al. , Phys. Rev. A, **66**, 21802(R)(2002).

[17] TOPAS laser tech. spec., Quantronix Scientific, www.quantronixlaser.com